Int J Adv Manuf Technol (2004) 23: 419–428
DOI 10.1007/s00170-003-1898-1

ORIGINAL ARTICLE

Y. Choi · R. Narayanaswami · A. Chandra

Tool wear monitoring in ramp cuts in end milling using the wavelet transform

Received: 11 March 2002 / Accepted: 20 May 2002 / Published online: 20 December 2003

Abstract Tool wear identification and estimation present a fundamental problem in machining. With tool wear there is an increase in cutting forces, which leads to a deterioration in process stability, part accuracy and surface finish. In this paper, cutting force trends and tool wear effects in ramp cut machining are observed experimentally as machining progresses. In ramp cuts, the depth of cut is continuously changing. Cutting forces are compared with cutting forces obtained from a progressively worn tool as a result of machining. A wavelet transform is used for signal processing and is found to be useful for observing the resultant cutting force trends. The root mean square (RMS) value of the wavelet transformed signal and linear regression are used for tool wear estimation. Tool wear is also estimated by measuring the resulting slot thickness on a coordinate measuring machine.

Keywords Cutting forces · Ramp cuts · Signal processing · Tool wear and Wavelet transform

1 Introduction

Monitoring cutting forces and tool wear effects in end milling is a necessary step toward the full automation of milling operations. To monitor the end milling process successfully, the selection of an appropriate signal and signal processing algorithm is very important. Several signals in a milling operation have been considered for monitoring tool failure, for example, cutting force, torque, vibration, acoustic emission, and spindle motor current.

This paper is concerned with monitoring the cutting force in ramp cuts in end milling. The ramp cuts are unique in that they have: (1) variation in the depth of cut and (2) the cutting force trends also depend on the feed direction [1]. Extensive experimental results have been observed progressively as new tools are being worn during machining, rather than focusing on new and/or broken (or pre-worn) tools.

The traditional signal processing approaches, such as segmental averages and Fourier transforms, generally assume that the sensor signals are constant. However, the sensor signals in tool wear monitoring usually vary. Thus, approaches that deal with varying signals are more appropriate for process monitoring. The wavelet transform is a convenient tool for processing time varying signals [2]. The wavelet transform is better suited than the Fourier transform for monitoring the cutting force as it provides time frequency localisation of the signal. The Fourier transform has a problem in that it transforms the signal from a time domain to a frequency domain, assuming that the signals are constant or infinite in nature [3]. However Fourier transforms have problems with describing transient components and do not convey any information pertaining to the translation of the signal from the time domain to the frequency domain. Accordingly, the wavelet transform is used to analyse the force signal.

The rest of the paper is organised as follows. First, a brief background on process monitoring, tool wear and cutting force modelling is provided. The experimental setup used to make the ramp cuts is described next. A short section on the wavelet transform for signal processing is included. Experimental data, explanation of trends in cutting force, effect of tool wear and its estimation with linear regression and metrology with a coordinate measuring machine (CMM) are provided next. Finally, conclusions and future research directions are presented.

Y. Choi · R. Narayanaswami (✉) · A. Chandra
Industrial and Manufacturing Systems Engineering,
Mechanical Engineering,
Iowa State University,
2019 Black Engineering Building,
Ames, IA 50011, USA
E-mail: ranga@iastate.edu

2 Related work

The monitoring of tool failure and tool wear has been the subject of active research. Tool wear is a complex phenomenon occurring in different metal cutting processes. Generally, worn tools adversely affect the surface finish of the workpiece and therefore there is a need to develop tool wear condition monitoring systems that alert the operator to the state of the tool, thereby avoiding undesirable consequences.

The cutting force signal provides rich information for tool failure detection in end-milling operations and in drilling [4]. For process monitoring purposes, segmental averages and Fourier transforms have been used extensively. However, the wavelet transform is increasingly being used for process monitoring. Wavelet transforms have two advantages over segmental averaging [5]: first, they represent the system more accurately if the waveforms are optimised by considering signal characteristics. Secondly, wavelet parameters can be used for many other purposes such as identification of tool breakage, run out and flute deviation. Tansel et al. [6] used both segmental averaging and wavelet transforms as encoding methods for tool wear estimation and found the wavelet transform to be superior. Wavelet transformations require less computation than fast Fourier transforms (FFT). For example, FFT requires $N \log_2 N$ operations for the transformation of a set of N numbers, while fast wavelet transformations require N operations and the number of operations halves when the transformations are repeated. Tansel et al. [7] studied the characteristics of normal and broken tool signals in end-milling operations with wavelet approximation coefficients. They observed that the variation of the estimated parameters of the wavelet transformations is very distinctive at different cutting conditions and when the tool is broken.

Gong et al. [8] estimated tool wear in turning operations with wavelet transform based on the cutting force. Wang, Mehrabi and Kannatey-Asibu [2] used a vibration signal and the wavelet transform to monitor tool wear in turning. They found the vibration signals from sharp and worn tools showed clear differences. A recent review of tool wear condition monitoring in turning with particular emphasis on using the acoustic emission (AE) signal may be found in [9]. Lee and Tarng [10] used spindle motor current to monitor tool failure in end milling. They used a wavelet transform to perform a multilevel signal decomposition to extract the tool failure feature and found the four-level wavelet decomposition to be adequate (decomposition up to the fourth level). Li and Wu [11] used wavelet analysis and AE signals in boring to monitor the tool wear state.

Li et al. [12], devised a tool breakage detection system for drilling, based on sensor fusion of AE and electrical current sensors. They found that the discrete wavelet transform could clearly diagnose tool breakage. Mori et al. [13] remarked that to predict drill bit breakage, it is necessary to detect and distinguish the signal behaviours that indicate pre-failure phenomena. They proposed a method for extracting pre-failure information from the cutting force to predict the breakage of a small drill bit. Li [14] also used the a.c. servo motor current signal and the wavelet transform to detect breakage of small diameter drills, while Li et al. [15] used wavelet transforms and fuzzy techniques to monitor tool breakage and wear conditions according to the measured spindle and feed motor currents.

Tool wear estimation under different cutting conditions is important to allow for increases in cutting force and other effects such as vibration. The cutting force models, which mainly model the cutting force under ideal conditions, can then be suitably modified and used in simulation and model-based process monitoring. Tool wear estimation can also lead to optimal tool usage by changing the tool at the most appropriate time.

The modelling of cutting forces in machining has been extensively studied and a recent review may be found in [16]. The mechanistic approach for modelling of cutting force has been successful. The mechanistic method views the machining process as a combination of the chip load solidus cutting force relationship, cutting tool geometry, cutting process geometry, workpiece geometry, and machining conditions.

The end-milling process has been modelled mechanistically [17] and EMSIM software [18] simulates forces in end milling. To obtain a complete representation of the forces on an end mill at any given instant, the cutter is discretised into thin, disk-like sections, similar to a stack of coins. The location of each flute on each disk is determined and the elemental force is calculated for each flute that engages the workpiece. The instantaneous chip thickness, the flute entry angle and the exit angle are needed in order to compute elemental cutting forces. For a small feed per tooth compared to the radius of the cutter, the instantaneous chip thickness is calculated as

$$t_c(i,j,k) = f_t \sin\beta(i,j,k) \tag{1}$$

Where, β is the wrap around angle due to the helix angle, and i, j, and k refer to the ith angular increment, jth axial height, and kth flute and f_t is the feed per tooth. The expressions for the elemental force acting normal to the rake face dF_N, and the friction force dF_T, are:

$$\begin{aligned} dF_N(i,j,k) &= K_N * dZ * t \\ dF_T(i,j,k) &= \mu * dF_N \end{aligned} \tag{2}$$

Where, dZ is the disk thickness, and the coefficients K_N and μ are determined experimentally by running a series of end milling or turning experiments and measuring forces for each workpiece/tool material combination. Once the normal and friction forces are calculated for a given element, they are transformed from the K_N-μ coordinate system to the X-Y-Z coordinate system. The total force is found by integrating the elemental forces. A comprehensive modelling of end-milling forces for arbitrary cutter geometry may be found in [19].

Advances have been made in incorporating the effect of tool wear in cutting force modelling. Elanayar and Shin [20] developed a method to separate the ploughing forces from the shear forces on the shear plane. The forces are decomposed by first separating the shear forces from the total forces and then employing an iterative procedure to calculate the normal forces on the shear plane. The ploughing forces are modelled by taking into account the change in geometry with flank wear. Smithey et al. [21] observed experimentally that in 3D cutting operations in which the nose of the tool is engaged, the region of plastic flow grows linearly as the total wearland width increases. Plastic flow occurs at the front of the wearland and elastic contact is assumed at the back of the wearland. The flank of the tool is discretised into small 2D elements and a contact model is used to determine the stresses on the individual elements. These stresses are added to the mechanistic force model for a sharp tool to determine the total cutting force.

From the literature it is evident that wavelet based signal analysis has been successful in tool breakage detection and also in the estimation of tool wear. Detailed wavelet coefficients have been used for breakage detection, particularly in drilling [4, 12, 13, 14, 15] and wavelet approximation coefficients have been used in monitoring tool wear in end milling [5, 6, 7, 10]. In previous work in the literature, tool wear has been estimated by comparison with pre-worn tools. There is no documented work on the estimation of progressive tool wear using the wavelet transform as the machining cuts are carried out. Further, the depth of cut within a machining cut has usually been taken as a constant, whereas this study used a variable depth of cut. Both these features make the work in this paper new. The estimation of tool wear in ramp cuts in end milling is carried out in this work by applying the wavelet transform to the resultant cutting force signal. The incorporation of progressive tool wear effects into a mechanistic model for cutting force modelling is a rich area that the authors are beginning to explore.

3 Experimental setup

As shown in Fig. 1a, a dynamometer is mounted on the table of a three-axis Fadal CNC machining centre. The workpiece is fixed in the vice, which is bolted to the top of the dynamometer. The DAQ card has 16 channels and a (-10 V $\sim +10$ V) display range. The amplifier has 3 channels to send data to the DAQ card for each x, y, and z force signals. The sampling rate is set at 500 Hz.

Ramp cut machining was carried out with a high-speed steel end mill on an AISI1018 steel workpiece (see Table 1). The workpiece and cut configuration is shown in Fig. 1b. Two types of ramp cut were machined as shown in Fig. 2 and are referred to as: (1) Low to high forward and (2) Low to high backward. The terms low and high refer to the axial depth of cut and the terms forward and backward refer to the tool feed direction.

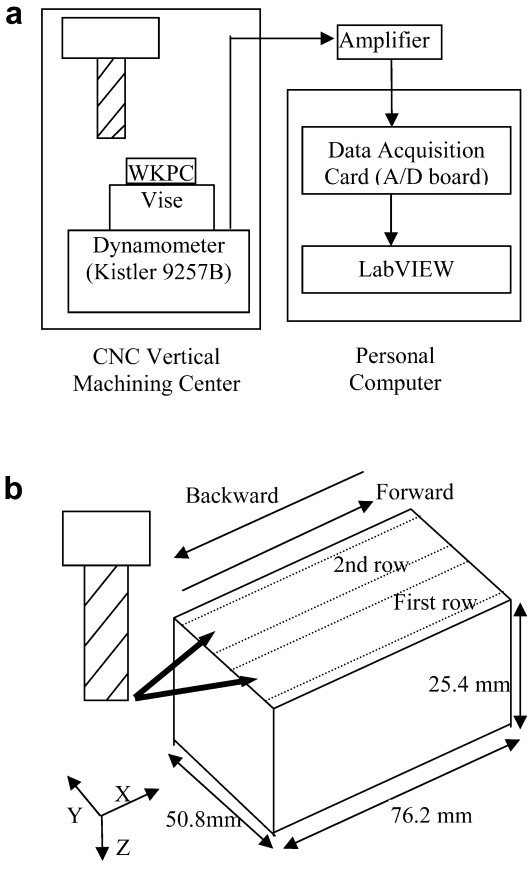

Fig. 1a, b Experimental set up and machining. **a** Schematic diagram of experimental set up. **b** Schematic diagram of machining

Table 1 Experimental conditions

Workpiece	AISI 1018 steel 50.8 mm×76.2 mm×25.4 mm
Tool	High-speed steel (12.7 mm/0.5 in diameter flat end mill with 4 flutes)
Depth of cut	0–1.27 mm, 0–2.54 mm, and 0–3.81 mm for ramp cut
Feed rate	25.4 and 50.8 cm/min
Spindle speed	1000 and 2000 rpm (CW)

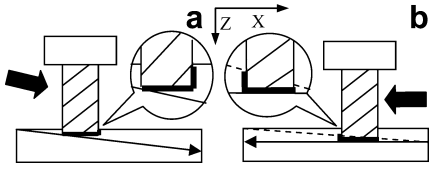

Fig. 2a, b Two types (low to high) of ramp cuts and their contact area between tool and workpiece. **a** Forward (odd) cut. **b** Backward (even) cut

As shown in Fig. 1b, at first the tool moves in the forward direction to create a forward ramp cut. Cutting force data is recorded and then the tool is moved in the backward direction to create the backward ramp cut. Repeated forward and backward cuts are made until the bottom of the workpiece is reached. Experimental

Table 2 Machining parameter sets

Cutting conditions	Depth of cut (mm)	Feed rate (cm/min)	Spindle speed (rpm)
1	0–1.27	25.4	1000
2	0–1.27	50.8	1000
3	0–2.54	25.4	1000
4	0–2.54	50.8	2000
5	0–3.81	25.4	1000

conditions used for the ramp cuts are shown in Table 1. Specific cutting conditions and parameters used for the ramp cuts are displayed in Table 2. Three choices of DOC (depth of cut), two values of feed rate and two values for the RPM were tried.

The target is to make 12 rectangular slots/6 workpieces (2 slots in each workpiece) by making ramp cuts. The size of each slot is 12.7 mm×76.2 mm×22.9 mm. To achieve this target with the conditions mentioned above, the required machining time and cut numbers are different. Cutting conditions 1 and 2 require 432 cuts to machine 12 slots (36 cuts in each slot) while cutting conditions 3 and 4 require 216 cuts (18 cuts in each slot) and cutting condition 5 needs 144 cuts (12 cuts in each slot). The required machining time for cutting conditions 2 and 4 is half of that for cutting conditions 1, 3, and 5 owing to the feed rate being faster by a factor of two. It is noted that the cutting forces shown in this paper are all in pounds.

4 Wavelet transform

Wavelets are a class of function that are the basic functions for a wavelet transform. Wavelets have proved useful in the analysis of signals that contain transients, image analysis, and image/signal compression. The wavelet transform decomposes a signal into a representation that shows signal details and trends as a function of time. This representation can be used to characterise transient events, reduce noise and many other applications. The wavelet transform maintains a constant time resolution regardless of frequency [3].

For many signals, the low-frequency content reflects the general trend, whereas the high-frequency content usually shows details of the process. In a wavelet transform, there are approximations and details. The approximations are the high-scale (low frequency) components of the signal and the details are the low-scale (high-frequency) components. Figure 3 shows the decomposition of a signal into approximations and details.

5 Experimental data and observations

Experimental data are presented for all five machining parameter sets for each forward and backward ramp

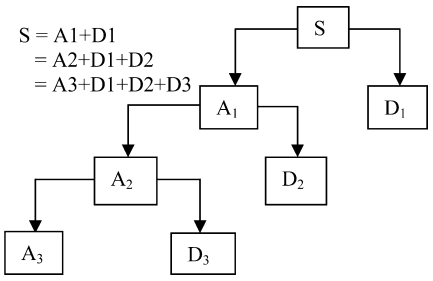

Fig. 3 Wavelet decomposition of a signal

cut. Cutting forces in the X-, Y- and Z-direction are measured. The $+X$-direction is the forward feed direction. The $+Z$-direction points downward. The $+Y$-axis forms a left-handed coordinate system. The resultant cutting force is obtained as shown in Eq. 3. A Daubechies wavelet transform is applied to the force data. The tool is assumed to be rotating in a clockwise direction.

$$\text{Resultant force} = \sqrt{(X^2 + Y^2 + Z^2)} \tag{3}$$

In each machining set the forward ramp cuts have odd numbers and the backward ramp cuts have even numbers. The process for forward and backward machining is repeated until 12 slots are machined in each machining condition.

Figure 4 shows the X, Y, and Z and the resultant cutting force for both the forward and backward ramp cut for a particular machining condition. All signals show either increasing or decreasing trends in cutting force, since the DOC in ramp cuts is either increasing or decreasing. These trends are not noticed in straight slot machining as the DOC is fixed. The cutting force trends for forward and backward cuts tend to be different as noted by Choi and Narayanaswami [1].

For the forward ramp cut, the X force increases continuously with increasing axial depth of cut. The Y force signal shows a downward sloping trend. It starts from the positive side of the axis at the first stage and tends to go to the negative side after the tool moves into the second half of the workpiece. The Z force is downward sloping and also may cross the axis.

For the backward ramp cut, the X force continuously decreases (increases in negative direction). The Y force signal shows an upward sloping trend (tool feed direction reversed). The Z force is downward sloping and crosses the axis.

The difference in cutting force trend between Figs. 4a and 4e is obvious. The crossing of the axis for the Y force in Fig. 4b needs some explanation. As can be seen from Fig. 2a and with respect to the bottom tool surface, both front and rear teeth (rear teeth with unit depth of cut) are engaged in machining for the forward ramp cut. For the backward ramp cut, however, only the front teeth are engaged in machining and rear teeth are contacting the workpiece surface without active machining.

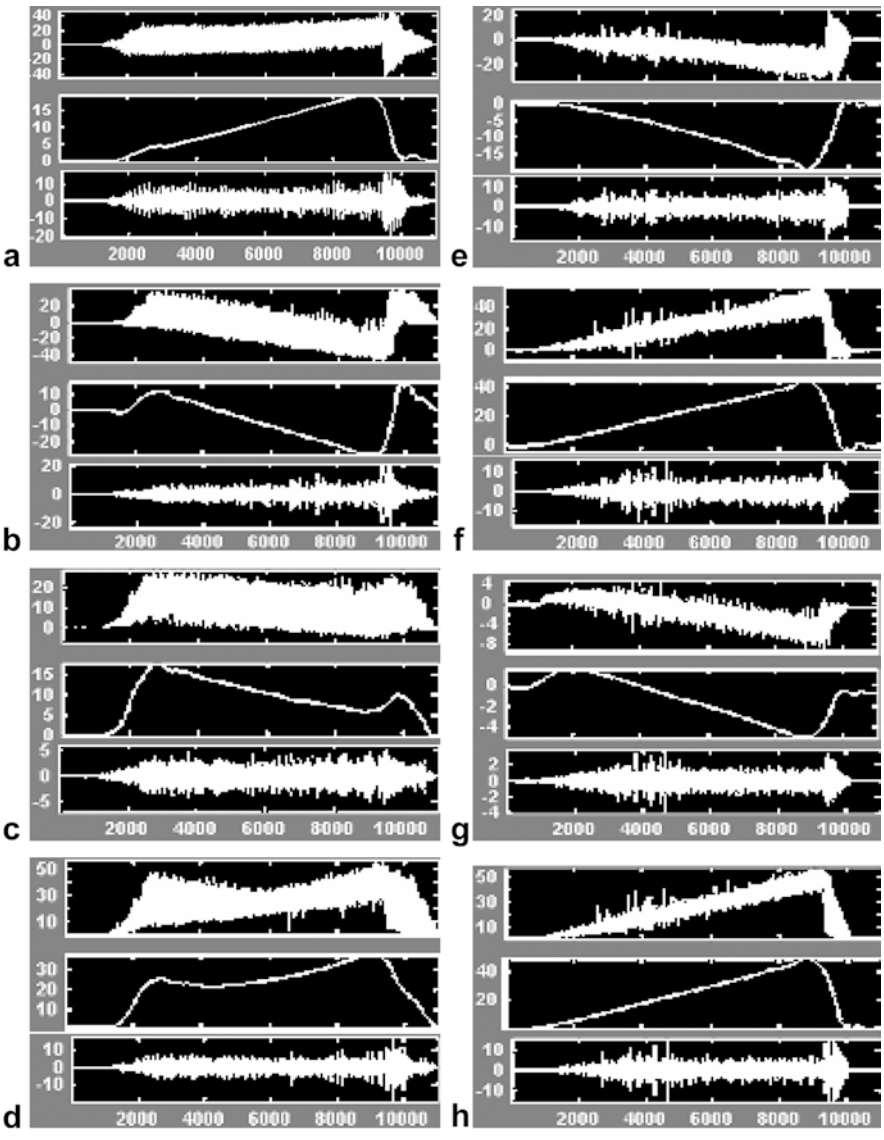

Fig. 4a–h *X*, *Y*, *Z*, and resultant force signals (lbs) for forward and backward machining (machining parameters of 0 to 1.27 mm DOC, 25.4 cm/min feed rate, 1000 rpm, and total 432 cuts)

Based on tool contact for the forward ramp cut, the key point to be noted is that teeth at the back are cutting only a unit amount of volume (principally at the bottom of the teeth). However, the teeth at the front side are removing more chips with both the sides and bottoms of the teeth as the tool moves down. The rear teeth provide the positive *Y*-force and the front teeth provide the negative *Y*-force. Therefore, as the depth of cut increases, the negative *Y* force exceeds the positive *Y* force. The *Y* signals therefore show the trend of crossing the axis to the negative side.

The *Z*-force trend for both forward and backward cuts also needs some more explanation. In Fig. 5a, it can be seen that '*I*' is the force due to the uniform downward pressure exerted by the bottom teeth of the tool and is independent of the depth of cut. The side cutting teeth on the front of the cutter are exerting an upward force (direction of chip exit), and as the axial depth of cut increases, the magnitude of this force increases. This is the negative *Z* force (II) in Fig. 5a. The net *Z* force is the summation of I+II. So "I+II" can cross the axis depending on the depth of cut. In Fig. 4c, the *Z* signal did not cross the axis because '*I*' was sufficiently large enough. In Fig. 4g the *Z* force crosses the axis and allows us to deduce that the downward pressure (*i*) is smaller in this case than the corresponding forward ramp cut because the tool does not contact the workpiece (Fig. 5b).

In summary, the forward and backward ramp cuts have different trends in cutting force because of differences in tool contact. In the case of the forward ramp cut, the back teeth on the bottom surface of the cutting tool are performing some cutting. Moreover, the downward thrust force or pressure exerted by the cutting tool is greater in the case of the forward ramp cut, as the tool is pressing down in the $+Z$ direction. So the resultant cutting force (RMS or mean) in forward machining is higher than the cutting force in backward machining, particularly for larger depths of cut.

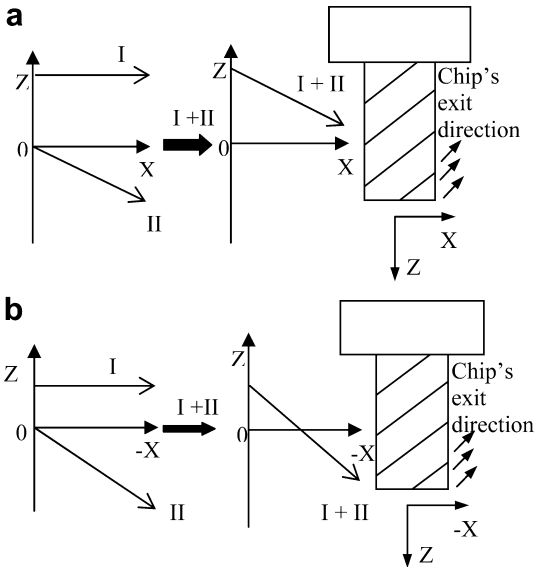

Fig. 5a, b Explanation of *Z* force signal for ramp cut. **a** Forward machining. **b** Backward machining

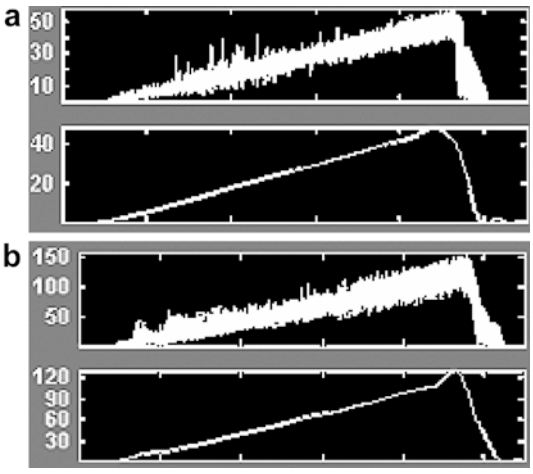

Fig. 7a, b Sample resultant force signals (lbs) for ramp cuts and their A9 s (machining parameters of 0 to 1.27 mm DOC, 25.4 cm/min^{-1} feed rate, 1000 rpm, and total 432 cuts)

6 Wavelet based signal processing of cutting force

The signal for one revolution of the tool is shown in Fig. 6. Thirty data points correspond to one revolution of the tool with a sampling rate of 500 Hz and a spindle rpm of 1000 rev_{min}. The figure displays two graphs of cutting force each with four peaks and four valleys corresponding to a four-fluted end mill. The graph with the lower magnitude peaks corresponds to the entry region of the cut (lower depth of cut) and the graph with the higher magnitude peaks corresponds to the exit region of the cut (higher depth of cut). As the depth of cut increases, it is observed that both the mean cutting force (approximation) and its oscillation (detail) increase.

6.1 Approximation coefficients

Figure 7 shows the resultant cutting force (RF) and its wavelet approximation coefficients at approximation level 9 (A9) as an example. A clear comparison is shown between an initial cut, cut number 4, (Fig. 7a) when the tool is new and the last cut, cut number 432 (Fig. 7b) when the tool is worn. From Fig. 7 it is clear that the cutting force increases within each cut and also the cutting force magnitude increases considerably with tool wear. The wavelet approximation A9 clearly shows the cutting force trend by filtering out the oscillations. The oscillations are captured by the detail wavelet coefficients.

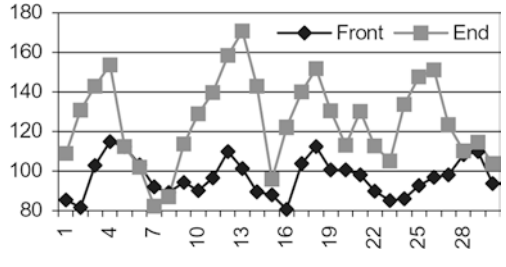

Fig. 6 Sample resultant force signal (lbs) for one revolution of the tool with scan rate of 500 Hz and spindle RMP of 1000 (cut number 215 of cutting condition 3)

The RMS value of the A9 coefficients within each cut is calculated as shown in Eq. 4. The RMS value of A9 within each cut is shown in Fig. 8, along with a linear regression fit. Figure 8 has 10 sub-graphs covering forward and backward machining cuts for all 5 experimental conditions.

$$RMS = \sqrt{\left(\frac{\sum_{i=1}^{n} x_i^2}{n}\right)} \qquad (4)$$

x = values of A9s

n = number of data

In Fig. 8, the *X*-axis represents the cut number and the *Y*-axis represents the RMS value of the resultant cutting forces at A9 at each graph. Data marked on the graphs are for cut number 3 or 4 (depending on forward or backward) and bottom cuts at each slot for both forward and backward cuts. The range of cut numbers in each subplot in Fig. 8 is different accordingly.

In all cases except two, Fig. 8g and 8i, the measured data fit into the linear equations well. Figures 8g and 8i both represent forward machining cuts with a higher DOC compared to machining parameter sets 1 and 2 making them somewhat severe machining conditions. As explained earlier, the forward ramp cuts generate more cutting force, and with larger DOC a linear regression is not appropriate. For high DOC forward ramp cuts, the cutting force is expected to have a non-smooth trend (locally) as shown in Figs. 8g and i, and with an increasing trend overall as machining continues.

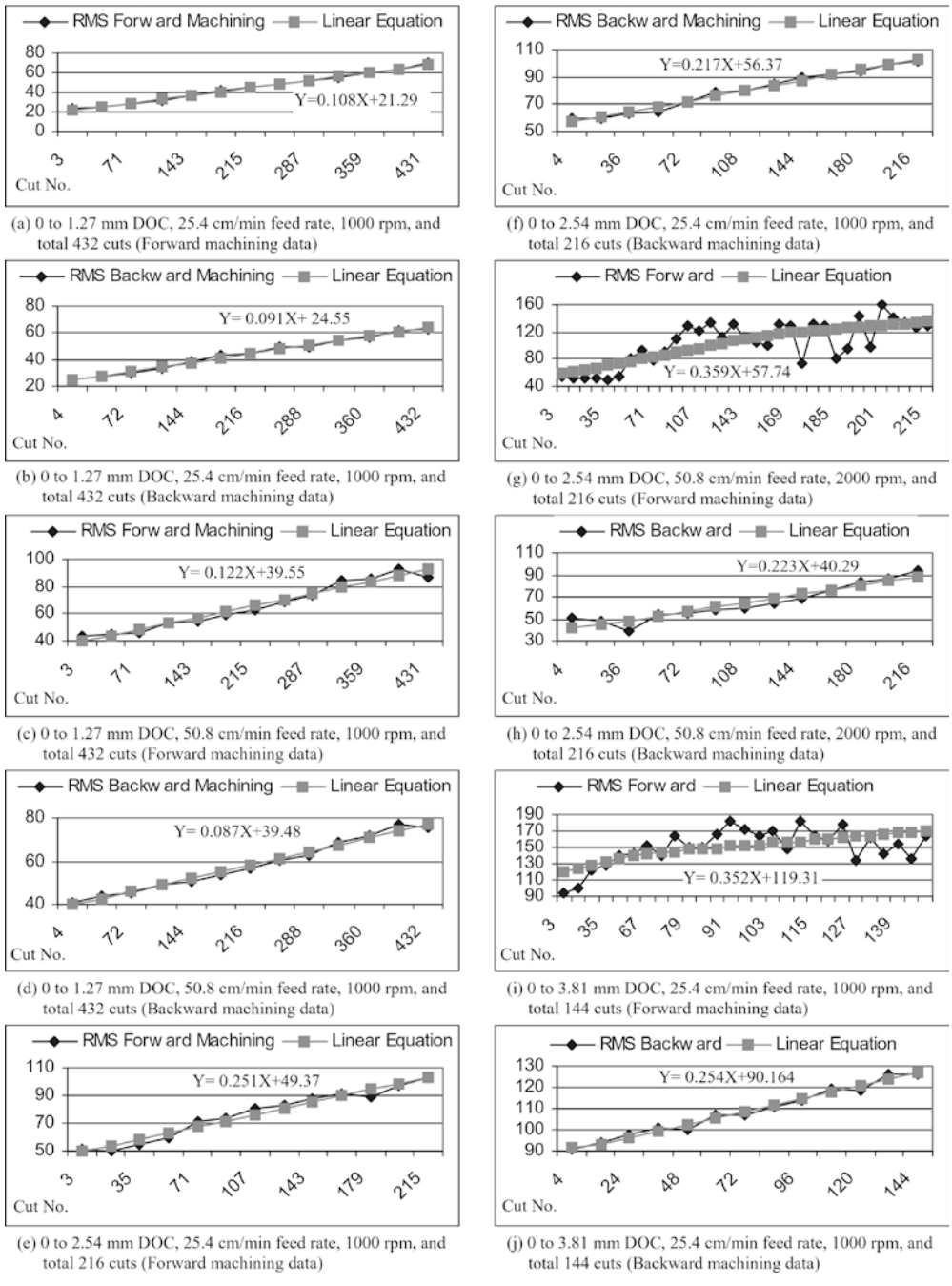

(a) 0 to 1.27 mm DOC, 25.4 cm/min feed rate, 1000 rpm, and total 432 cuts (Forward machining data)

(b) 0 to 1.27 mm DOC, 25.4 cm/min feed rate, 1000 rpm, and total 432 cuts (Backward machining data)

(c) 0 to 1.27 mm DOC, 50.8 cm/min feed rate, 1000 rpm, and total 432 cuts (Forward machining data)

(d) 0 to 1.27 mm DOC, 50.8 cm/min feed rate, 1000 rpm, and total 432 cuts (Backward machining data)

(e) 0 to 2.54 mm DOC, 25.4 cm/min feed rate, 1000 rpm, and total 216 cuts (Forward machining data)

(f) 0 to 2.54 mm DOC, 25.4 cm/min feed rate, 1000 rpm, and total 216 cuts (Backward machining data)

(g) 0 to 2.54 mm DOC, 50.8 cm/min feed rate, 2000 rpm, and total 216 cuts (Forward machining data)

(h) 0 to 2.54 mm DOC, 50.8 cm/min feed rate, 2000 rpm, and total 216 cuts (Backward machining data)

(i) 0 to 3.81 mm DOC, 25.4 cm/min feed rate, 1000 rpm, and total 144 cuts (Forward machining data)

(j) 0 to 3.81 mm DOC, 25.4 cm/min feed rate, 1000 rpm, and total 144 cuts (Backward machining data)

Fig. 8a–j Linear regression of root mean square of A9s of resultant cutting forces (lbs)

The graphs in Fig. 8 can be compared with respect to changes in the machining conditions. Graphs for forward machining, Figs. 8a, e, and i, show that the RMS maximum and minimum values of RMS clearly increased with increased DOC while maintaining other cutting conditions the same. The same trend is also noticed for backward machining cuts as shown in Figs. 8b, f, and j where the depth of cut is increased and other cutting conditions are the same.

The effect of feed rate is another important parameter to be observed. A comparison between Figs. 8a and c for forward cuts and between Fig. 8b and d for backward cuts, where the feed rate is doubled, indicates that cutting forces have increased with increase in feed rate.

Cases shown in Fig. 8g and h are difficult to compare directly to other graphs since they have changes in two different conditions (increased rpm) and feed rate as compared to other graphs.

6.2 Detail coefficients

The importance of maintaining details in the wavelet transform is to capture any discontinuities in the frequency that occurs within the time domain. Disconti-

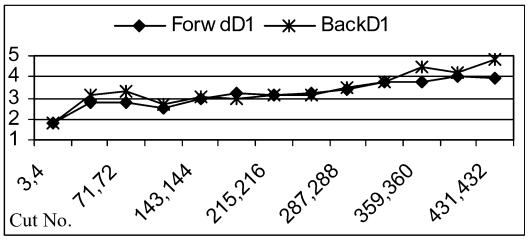

(a) 1.27 mm DOC, 25.4 cm/min feed, and 1000 rpm

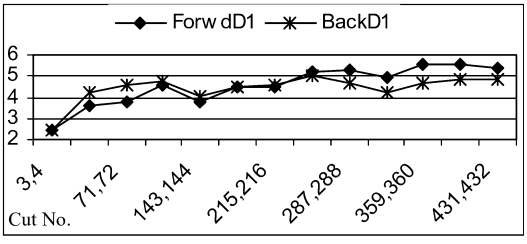

(b) 1.27 mm DOC, 50.8 cm/min feed, and 1000 rpm

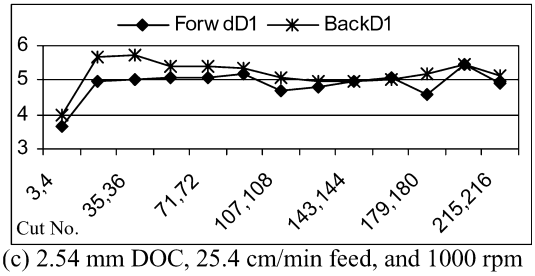

(c) 2.54 mm DOC, 25.4 cm/min feed, and 1000 rpm

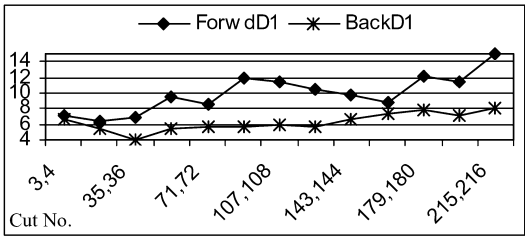

(d) 2.54 mm DOC, 50.8 cm/min feed, and 2000 rpm

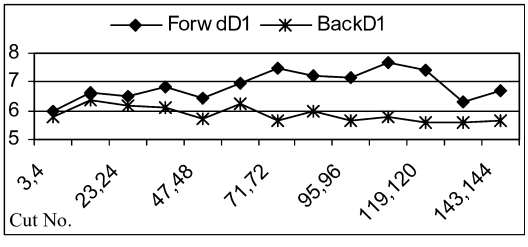

(e) 3.81mm DOC, 25.4 cm/min feed, and 1000 rpm

Fig. 9a–e RMS of D1 for each machining set (lbs)

nuities may occur in the event of a cutting edge being chipped or broken, for example. The details will show these phenomena, while the approximations will still reflect tool wear. Other process faults such as run out and flute deviation, can further complicate the signal and an entire set of wavelet coefficients is necessary to handle the many process faults, tool wear and the possibility of tool chipping or breakage in order to establish a reliable process monitoring system [1].

The RMS values of the detail coefficients at level 1 are displayed in Fig. 9. The *X*-axis shows cut numbers at each machining condition and the *Y*-axis shows the RMS value of the detail coefficients. Each subfigure has two graphs for forward and backward machining. One trend to notice is that detail coefficients increase with increased feed rate or DOC. A higher detail value means higher oscillation of the original signal. In Figs. 9a, b and d there is a gradual increase in the value of the detail coefficient. This is suggestive of larger cutting force oscillation as a result of tool wear. These trends are not so noticeable in Figs. 9c and e.

7 Tool wear

Fig. 8 shows that repeated machining with the same tool leads to an increase in the cutting force as a result of tool wear. The wavelet approximations of the resultant forces show an increase in the mean force of ramp cuts, as shown in Fig. 7. A sample SEM picture of one side flute of the worn tool is shown in Fig. 10. The amount of tool wear may be estimated using linear regression as well as metrology of the machined slot. Both of these are considered below.

7.1 Tool wear estimation with linear regression

The value of 1.0 minus residual variance is referred to as *R*-square or the coefficient of determination. The *R*-square value is an indicator of how well the model fits the data (e.g. an *R*-square close to 1.0 indicates that almost all of the variability has been accounted for with the variables specified in the model). Table 3 shows all the *R*-squares of the linear regression in Fig. 8. All values are close to 1.0 except for Fig. 8g and i, where linear regression is not appropriate.

As can be seen from Table 4, each linear equation fits the measured value of the RMS well. Only machining parameter sets 1, 2, and 3 have been tested since sets 4 and 5 are considered somewhat severe conditions. The maximum difference between measured and linear

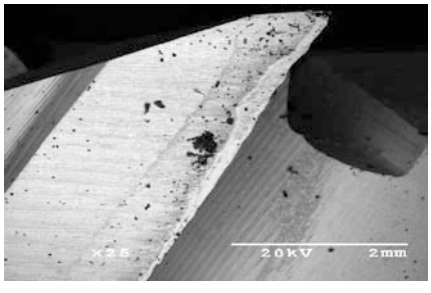

Fig. 10 Sample SEM photograph of a single flute of a worn 4 fluted end mill

Table 3 *R*-squares of linear regressions in Fig. 8

Cutting conditions	Sub-figures	*R*−square
1.27 mm, 25.4 cm/min,	(a)	0.993
1000 rpm, and 432 cuts	(b)	0.991
1.27 mm, 50.8 cm/min,	(c)	0.964
1000 rpm, and 432 cuts	(d)	0.985
2.54 mm, 25.4 cm/min,	(e)	0.969
1000 rpm, and 216 cuts	(f)	0.985
2.54 mm, 50.8 cm/min,	(g)	0.578
2000 rpm, and 216 cuts	(h)	0.900
3.81 mm, 25.4 cm/min,	(i)	0.407
1000 rpm, and 144 cuts	(j)	0.983

equation of RMS is 5.38%. Two cut numbers, for both forward and backward cuts for each machining parameter set, were selected randomly and tested.

7.2 Metrology

A coordinate measuring machine (CMM) was also used to estimate the tool wear. For each machining set, first the slot width at the top part of the first workpiece is measured (very first machining) and then the slot width at the bottom of the cut for each workpiece in consecutive order is measured next. These slot sizes are compared relative to the initial size of the first measurement (at the top of the first workpiece). Results are shown in Table 5.

For each machining parameter set, the slot width is reduced from the first cut to the last cut. This is indicative of tool wear. It can be seen that as the machining conditions become more severe with higher feed rate or DOC, the amount of tool wear is increasing (slot size is become smaller). Machining parameter set 5 is the most severe machining condition (highest tool wear). The measured slot width can therefore also serve as an indicator of tool wear and can be used as an indicator for tool changing.

8 Conclusions and future work

Experimental cutting force data in ramp cuts in end milling were generated and analysed for tool wear effects. The ramp cuts are unique in that they have a changing depth of cut. A wavelet transform was used to generate a multilevel decomposition of the cutting force signal. Cutting force trends have been observed progressively as new tools are worn using different cutting parameters. The RMS value of the approximation coefficients of the resultant cutting force signal was used to model and estimate tool wear. For smaller depths of cut, a linear regression fit of the RMS value of the approximation coefficients was obtained. Under these conditions, tool wear was estimated within an error of 6%. Metrology was also used to estimate the tool wear. The slot thickness is continuously reduced as the tool is worn and can serve as another indicator for tool wear estimation.

The estimation of tool wear can be used to plan optimal tool replacement. The addition of tool wear into existing cutting force models presents an interesting future research direction. The next phase of the work will involve mechanistic modelling of the cutting force, including the effect of tool wear. This will result in an effective model-based tool monitoring system for end milling that can be useful in industry. The new mechanistic model of cutting force may be used in simulations and in planning optimal tool replacement.

Acknowledgement This research is supported by the National Science Foundation under grant no. DMI 9970083. Any opinions, findings, and conclusions or recommendations expressed in this material are those of the authors and do not necessarily reflect the views of the National Science Foundation. The authors gratefully

Table 5 Measurements of relative slot thickness (mm) using a CMM

Cutting conditions	Locations	Relative slot thickness
1.27 mm, 25.4 cm/min,	Bottom at 3rd wkpc	−0.0457
1000 rpm, and 432 cuts	Final size	−0.0483
1.27 mm, 50.8 cm/min,	Bottom at 3rd wkpc	−0.0559
1000 rpm, and 432 cuts	Final size	−0.0940
2.54 mm, 25.4 cm/min,	Bottom at 3rd wkpc	−0.1397
1000 rpm, and 216 cuts	Final size	−0.2388
2.54 mm, 50.8 cm/min,	Bottom at 3rd wkpc	−0.1575
2000 rpm, and 216 cuts	Final size	−0.2718
3.81 mm, 25.4 cm/min,	Bottom at 3rd wkpc	−0.1829
1000 rpm, and 144 cuts	Final size	−0.2921

Table 4 Comparison of measured RMS of resultant force at A9 and linear regression models

	Direction	Cut number	Measured	Linear Equtation	Difference %
DOC: 1.27 mm	Forward	63	27.4868	28.094	2.21
Feed: 25.4 cm/min		235	47.5376	46.67	−1.83
Speed: 1000 rpm	Backward	100	33.2808	33.65	1.11
Total 432 cuts		280	50.0618	50.03	−0.06
DOC: 1.27 mm	Forward	119	54.4915	54.068	−0.78
Feed: 50.8 cm/min		379	87.9340	85.788	−2.44
Speed: 1000 rpm	Backward	208	58.0055	57.576	−0.75
Total 432 cuts		416	75.7522	75.672	−0.11
DOC: 2.54 mm	Forward	31	54.6216	57.151	4.63
Feed: 25.4 cm/min		115	81.5575	78.235	−4.07
Speed: 1000 rpm	Backward	140	91.6803	86.75	−5.38
Total 216 cuts		190	100.2500	97.6	−2.64

acknowledge help from Jim Dautremont in Mechanical Engineering and Kevin Brownfield in Industrial and Manufacturing Systems Engineering for assistance with the machining experiments.

References

1. Choi Y, Narayanaswami R (2002) Experimental observations of cutting force and tool wear effects in ramp cuts in end milling. Trans NAMRI/SME 30 (in press)
2. Wang L, Mehrabi MG, Kannatey-Asibu Jr. E (2001) Tool wear monitoring in machining processes through wavelet analysis. Trans NAMRI/SME 29:399–406
3. Misiti M, Misiti Y, Oppenheim G, Poggi J (1996) Wavelet Toolbox. Mathwork Inc
4. Li X (1998) Real-time detection of the breakage of small diameter drills with wavelet transform. Int J Adv Manuf Tech 14:539–543
5. Tansel I, Rodriguez O, Trujillo M, Paz E, Li W (1998) Micro-end milling I: wear and breakage. Int J Mach Tool Manuf 38:1419–1436
6. Tansel IN, Arkan TT, Bao WY, Mahendrakar N, Shisler B, Smith D, McCool M (2000) Tool wear estimation in micro-machining, part II: neural-network-based periodic inspector for non-metals. Int J Mach Tool Manuf 40:609–620
7. Tansel IN, Mekdeci C, Mclaughlin C (1995) Detection of tool failure in end milling with wavelet transformations and neural networks. Int J Mach Tool Manuf 35(8):1137–1147
8. Gong W, Obikawa T, Shirakashi T (1997) Monitoring of tool wear states in turning based on wavelet analysis. JSME Int J 40(3):447–453
9. Li X (2002) A brief review: acoustic emission method for tool wear monitoring during turning. Int J Mach Tool Manuf 42:157–165
10. Lee BY, Tarng YS (1999) Application of the discrete wavelet transform to the monitoring of tool failure in end milling using the spindle motor current. Int J Adv Manuf Tech 15:238–243
11. Li X, Wu J (2000) Wavelet analysis of acoustic emission signals in boring. In: proceedings of the institution of mechanical engineers, part B. J Eng Manuf 214(5):421–424
12. Li X, Dong S, Yuan Z (1999) Discrete wavelet transform for tool breakage monitoring. Int J Mach Tool Manuf 39:1935–1944
13. Mori K, Kasashima N, Fu JC, Muto K (1999) Prediction of small drill bit breakage by wavelet transforms and linear discriminant functions. Int J Mach Tool Manuf 39:1471–1484
14. Li X (1999) On-line detection of the breakage of small diameter drills using current signature wavelet transform. Int J Mach Tool Manuf 39:157–164
15. Li X, Tso S, Wang J (2000) Real-time tool condition monitoring using wavelet transforms and fuzzy techniques. IEEE Transactions on Systems, Man and Cybernetics-Part C: Applications and Reviews 30(3):352–357
16. Ehmann KF, Kapoor SG, DeVor RE, Lazoglu I (1997) Machining process modelling: a review. J Manuf Sci Engineer 119:655–663
17. Devor RE, Kline WA, Zdeblick WJ (1980) A mechanistic model of the force system in end milling with application to machining airframe structures, Proceedings of the 8th North American Metalworking Research Conference, pp 297–303
18. "EMSIM,"http://mtamri.me.uiuc.edu
19. Altintas Y, Engin S (2001) Generalized modelling of mechanics and dynamics of milling cutters. Annals of the CIRP 50(1):25–30
20. Elanayar S, Shin YC (1996) Modelling of tool forces for worn tools: flank wear effects. J Manuf Sci Engineer 118(3):359–366
21. Smithey DW, Kapoor SG, DeVor RE (2000) A worn tool force model for three-dimensional cutting operations. Int J Mach Tool Manuf 40:1929–1950